Magnetic exchange interactions in the gadolinium pnictides from first principles

Chandrima Mitra and Walter R. L. Lambrecht
Department of Physics, Case Western Reserve University, Cleveland, Ohio 44106-7079, USA
(Received 13 August 2008; published 27 October 2008)

The magnetic exchange interactions in the Gd-pnictide series are analyzed from various points of view. First, a Heisenberg Hamiltonian between the 4*f* induced local moments on the Gd only is used and the corresponding exchange interactions between first and second-nearest neighbors are derived from total-energy differences between the ferromagnetic (FM) and antiferromagnetic AFM-I and AFM-II configurations, as calculated from a full-potential-linearized muffin-tin orbital method in the local-density approximation with Hubbard-*U* corrections (LSDA+*U*). The induced magnetic moments on Gd *d* and N in the different configurations are found to differ and to favor the AFM-II for the P-Bi compounds while the FM configurations is favored for GdN. The extracted J_2 parameter determines the Néel temperature of the AFM-II compounds in good agreement with experimental values. The Curie-Weiss temperature involves both J_1 and J_2 in this model and is also in good agreement with experiment. The FM state of GdN can be viewed as an antiferromagnetic arrangement of the small moments induced on Gd *d* and N on the rocksalt lattice, which in this case happen to cancel each other exactly because of the semiconducting nature of GdN. This locks the Gd 4*f* moments into a FM arrangement through the on-site *f*-*d* coupling. Linear response calculations in the atomic sphere approximation, including empty sphere sites, provide an alternative decomposition of the magnetic ordering energy in Gd-Gd, Gd-N, and Gd-empty sphere exchange interactions. The latter can be viewed as representing the tails of the t_{2g} orbitals on Gd. This analysis shows that the magnetic ordering arises from the small induced moments on the Gd *d*, N, and empty sphere sites rather than from direct interactions between 4*f* moments. The Curie temperature for GdN is found to be significantly smaller than previous calculations estimated and than experimental values and may indicate that the latter are influenced by defects. For GdP, GdAs, GdSb, and GdBi, the linear-response calculations around the AFM-II ground state give results in good agreement with the full-potential linearized muffin-tin orbital calculations. The linear-response approach also gives a reasonable value for the Curie temperature of metallic Gd.

DOI: 10.1103/PhysRevB.78.134421 PACS number(s): 71.70.Gm, 71.23.An

I. INTRODUCTION

Recently, there were several studies of the magnetic exchange interactions in the Gd pnictides: Gd *X*, with *X*=N, P, As, Sb, and Bi.[1–6] These materials all share the rocksalt structure. Except for GdN, they are all semimetallic and antiferromagnetic (AFM) with the AFM-II structure as ground state, i.e., ferromagnetically ordered (111) planes alter in spin orientation from layer to layer. We will denote this as $[111]_1$. GdN however is ferromagnetic (FM) and semiconducting.[7–10] Although most of the recent computational studies used local-spin-density approximation with Hubbard-*U* correction (LSDA+*U*), there is still no convergence on the magnitude of the exchange interactions or their interpretation in terms of simple models. Usually, a Heisenberg Hamiltonian is postulated for the interaction between the localized moments resulting from the half-filled 4*f* shell,

$$H = -\sum_{ij} J_{ij} \mathbf{S}_i \cdot \mathbf{S}_j. \tag{1}$$

While Li *et al.*[1] and Larson and Lambrecht[3] used $S=7/2$, some authors use a classical Heisenberg model, in which **S** becomes a unit vector. The only difference between both formulations is that J_{ij} of the former are smaller by a factor $S(S+1)=63/4$. Another slight difference between formulations is that some authors[1,3] take the sum in Eq. (1) to run over all *i* and *j* while others[4,5] sum each pair only once and hence differ by a factor 2. Here we will use the classical Heisenberg Hamiltonian and the convention of counting each pair only once, the same as that in Duan *et al.*[5] Even when renormalizing for these trivial changes in convention, the exchange interactions of Duan *et al.*[5] were smaller than those reported by Larson and Lambrecht[3] by about a factor 2.

In this paper, we first of all recalculate the energy differences between the AFM-I ($[001]_1$), AFM-II, and (FM) states using the full-potential linearized muffin-tin orbital (FP-LMTO) method,[11] from which we can then fit J_1 and J_2 using

$$\Delta E_{\mathrm{I}} = E(\text{AFM-I}) - E(\text{FM}) = 8J_1,$$

$$\Delta E_{\mathrm{II}} = E(\text{AFM-II}) - E(\text{FM}) = 6J_1 + 6J_2. \tag{2}$$

We find much better agreement for J_2 with the calculations of Duan *et al.*[5] which determine directly the Néel temperature. We also find better agreement with the experimental Curie-Weiss temperatures[1] extracted from susceptibility as a function of temperature than either of the two previous calculations.

Next, we discuss the nature of the magnetism in these systems. Duan *et al.*[5] already pointed out that J_2 correspond essentially to antiferromagnetic superexchange between Gd *d* via the intervening anion-*p* orbitals. Indeed, they showed it to be given approximately by

$$J_2^{\text{super}} = -n_d \frac{t_{pd}^2}{\Delta^2}\left[\frac{1}{\Delta}+\frac{1}{U}\right], \tag{3}$$

originally derived by Zaanen and Sawatzky,[12] in which t_{pd} is the p-d hopping integral, Δ is the charge-transfer energy between anion-p and cation-d levels, the on-site Coulomb energy U is implicitly assumed by Duan *et al.*[5] to be large relative to Δ and thus $1/U$ is neglected, and n_d is the d contribution to the magnetic moment. Without the first term this would correspond to Anderson's equation for superexchange with t_{pd}^2/Δ as the effective hopping between d orbitals via the intervening anion p's. Whether this limit is correct is somewhat questionable but in any case it only is meant to provide an insight into the results of the actual first-principles calculations in terms of well-known models of exchange interaction. This interaction increases in magnitude with the size of the group-V element. The magnetic moments on Gd d are induced by the f-d coupling. The nearest-neighbor interaction is interpreted by Duan *et al.*[5] as a carrier mediated [Ruderman-Kittel-Kasuya-Yosida (RKKY)] (Refs. 13–15) coupling of the local $4f$ moments in the conduction-electron gas. However, in pure semiconducting GdN, this interpretation does not hold; so where does the ferromagnetism in GdN come from? We will show that a detailed examination of the small induced magnetic moments on the N and Gd d holds clues. It allows us to describe the FM state of GdN as an "antiferromagnetic state in disguise" because opposite moments are found on Gd d and N and form a perfectly interlocking system.

Next, we use the linear-response approach of Liechtenstein *et al.*[16] in the atomic sphere approximation (ASA) to gain further insight in the nature of the exchange interactions. Although the latter is found to be not quite as accurate, it will be shown to provide an alternative description of the nature of the magnetic exchange interactions.

Finally, the net result of our study is that while good agreement is obtained with the Néel temperatures for Gd X with X=P, AS, Sb, and Bi, it gives a severe underestimate of the Curie temperature in GdN. This indicates that the experimental Curie temperatures in that system may be influenced by defects or other extrinsic causes.

II. COMPUTATIONAL METHODS

The basic approach of all our calculations is the density-functional theory[17,18] in the local-spin-density approximation (LSDA) (Ref. 19) but with orbital-dependent Coulomb and exchange integrals added, the so-called LSDA+U approach.[20,21] In this approach, the screened on-site Coulomb interaction U_f and the corresponding exchange interactions described in terms of the unscreened atomic parameter J_f of the localized f electrons are added at the unrestricted Hartree-Fock level and their orbital-independent average is subtracted to avoid double counting the terms already present in LSDA. We here also use the LSDA+U treatment for the Gd d electrons. Although the latter form a fairly wide band, they give rise to the conduction-band minimum. The usual LSDA underestimate of the gap in semiconductors and even semimetals can be corrected by slightly shifting up the d levels, which can be done by adding U_d because for empty states the LSDA+U method essentially shifts up the d-orbital energy by $U_d/2$. This approach was recently shown to work well for Gd pnictides[3] and other rare-earth nitrides.[22] The parameters used for U_f is the same as in Ref. 3 and chosen so as to reproduce the splitting between occupied and empty $4f$ states in the Gd pnictides as determined by x-ray photoelectron spectroscopy (XPS) and bremsstrahlung isochromat spectroscopy (BIS).[23] The parameter U_d is slightly different from that in Ref. 22, so as to accommodate the more recent information on the band gap in GdN.[8]

The calculations are carried out using the linearized muffin-tin orbital (LMTO) method,[24] both in the ASA (Refs. 25 and 26) and in a full-potential (FP) version.[11] The latter is more accurate in treating the potential because it makes no shape approximations. The former has the advantage that it is more closely connected to multiple-scattering theory and thus can be implemented in terms of the Green's functions.[25–27] In particular, this is useful to describe the exchange interactions in terms of linear response.[16,28] Convergence issues of the FP-LMTO in terms of **k** points, etc., are mentioned below as part of our discussion of the results.

III. RESULTS

A. Full-potential results

We begin by revisiting our FP-LMTO calculations in more detail. We use the FP-LMTO method[11] in the LSDA+U approach with U_f=8 eV and J_f=1.2 eV and an additional U_d=3.4 eV, J_d=0 exactly as in Larson and Lambrecht.[3] The relevant parameter for a half-filled shell is U_f-J_f=6.8 eV is slightly larger than the one used by Duan *et al.*,[5] U_f=6.7 eV, J_f=0.7 eV, and U_f-J_f=6.0 eV, who used the full-potential linearized augmented plane-wave (FLAPW) approach. Those authors did not use a U_d and hence obtain a semimetallic band structure for GdN, while we obtain a gap in agreement with recent experimental studies.[7,8] The only difference in our calculation with that of Larson and Lambrecht[3] is that we use a larger basis set, ($spdfg$,$spdf$) on Gd, meaning two sets of κ and smoothing radius for the smoothed Hankel functions for all l up to f and one for g orbitals, ($spdf$,sp) for the anion, and including Gd $5p$ as local orbitals,[29] larger augmentation angular-momentum cutoff $l_{\max}$=5. With such a large basis set the FP-LMTO method results are converged to be better than meV precision level required here and comparable to LAPW calculations as done by Duan *et al.*[5] A major difference from the previous work of Larson and Lambrecht[3] is that we use differently chosen supercells from which to extract the energy differences. We here used a doubled cell with lattice vectors $(-1/2,1/2,0)$, (1/2,1/2,0), and (0,0,1) in units of the cubic lattice constant a for $[001]_1$ and (1/2,1/2,0), (0,1/2,1/2), and (1,0,1) for $[111]_2$ and each time evaluates both the AFM and FM configurations of spins on each of those to calculate the relevant AFM-FM energy difference. This has the advantage that exactly the same **k**-point mesh and real-space mesh (for the smooth part of the charge density and potential) are used for the AFM and FM cases so that some cancellation of errors takes place. We also checked that by using a high

TABLE I. Magnetic energy differences (in meV/pair), Heisenberg exchange parameters (in meV), and Néel and Curie-Weiss temperatures (in kelvins).

	ΔE_{I}	ΔE_{II}	J_1	J_2	T_N (MF)	$0.7T_N$ (MF)	T_N (expt.)[a]	T_{CW}	T_{CW} (expt.)
GdN	3.4	0.4	0.42	−0.36			58	11	81.0
GdP	2.7	−2.9	0.34	−0.82	19	13	15.9	−3	4.0
GdAs	0.95	−5.5	0.12	−1.03	24	17	18.7	−18	−11.8
GdSb	1.2	−6.5	0.15	−1.22	28	20	23.4	−22	−31.3
GdBi	0.1	−8.4	0.01	−1.40	32	23	25.8	−32	−45.0

[a]T_C for GdN, the experimental values in this column and T_{CW} are from Li *et al.* (Ref. 1).

enough **k**-point convergence the two structures give the same FM energy to the required precision. To obtain absolute convergence of the FM energy, i.e., the same in both structures to 1 μeV, we needed a $16\times16\times16$ division. However, a **k**-point meshes of $6\times6\times6$ was found adequate to obtain the relevant AFM-FM energy differences converged to 0.1 meV.

The resulting energy differences and the extracted J_1, J_2, Néel, and Curie-Weiss temperatures are given in Table I. These were calculated at the experimental equilibrium lattice constant. For comparison we also calculated the same results at the theoretical equilibrium lattice constants obtained with our current basis set. The experimental and theoretical lattice constants and the corresponding J_1 and J_2 values are compared in Table II. The calculated equilibrium lattice constants are about 2% larger when using Gd $5p$ as local orbital. We can see that J_2 changes moderately by using the theoretical equilibrium lattice constant but J_1 becomes smaller and even changes sign. This would result in more negative Curie-Weiss temperatures.

In the mean-field approximation, the Néel temperature for the AFM-II configuration is given by

$$T_N(\mathrm{MF}) = -2J_2/k_B, \tag{4}$$

with k_B as Boltzmann's constant. Typically, the mean-field theory overestimates the actual Néel temperature by about 30%, as we can deduce by comparing the Monte Carlo results of Duan *et al.*[5] with the mean-field T_N(MF) deduced from their J_2. We thus use $T_N=0.7T_N$(MF) as our best estimate. The Curie-Weiss temperature T_{CW} on the other hand, given by the high-temperature form of the susceptibility, $\chi=A/(T-T_{\mathrm{CW}})$, is better described by mean-field theory and is given by

TABLE II. Exchange parameters with the experimental and theoretical lattice constants.

	a_{th} (Å)	a_{ex} (Å)	J_1 (theor.)	J_1 (expt.)	J_2 (theor.)	J_2 (expt.)
GdN	5.07	4.98	0.40	0.42	−0.34	−0.36
GdP	5.84	5.71	0.13	0.34	−0.82	−0.82
GdAs	6.00	5.86	−0.02	0.12	−0.96	−1.03
GdSb	6.39	6.22	−0.02	0.15	−1.28	−1.22
GdBi	6.43	6.3	−0.01	0.01	−1.99	−1.40

$$T_{\mathrm{CW}} = (4J_1 + 2J_2)/k_B. \tag{5}$$

For the ferromagnetic case, $T_{\mathrm{CW}}=T_{\mathrm{Curie}}$(MF). For the antiferromagnetic case, $T_{\mathrm{CW}}<0$.

Comparing with the results of Duan *et al.*,[5] we find slightly lower values for $|\Delta E_{\mathrm{II}}|$ but a different sign for ΔE_{I} for P-Bi. We obtain good agreement for J_2 but positive J_1 for Gd(P-Bi). Their values for J_1 are 0.86, −0.17, −0.22, −0.51, and −0.66 meV for the series from N to Bi. For J_2, their values are −0.14, −0.74, −0.91, −1.13, and −1.37 meV. This results in our estimates of Néel temperatures in excellent agreement with theirs and about 10%–20% below the experimental value. Our values for the Curie-Weiss temperatures are closer to the experiment than the values which we can extract from their parameters: 37, −25, −31, −50, and −62 K, respectively, for Gd(N-Bi). Li *et al.*[1] extracted J_1 and J_2 values from the mean-field equations for the Curie or Néel temperature and the Curie-Weiss temperatures. Their J_2 and J_1 values are −0.92, −0.95, −1.63, and −1.71 meV and 0.60, 0.22, 0.14, and −0.11 for Gd(P-Bi) after conversion to our present conventions of the classical Heisenberg Hamiltonian. For GdN, they only extract $J_1=1.74$ meV. The values from Larson and Lambrecht[3] are −0.87, −1.35, −1.52, −1.95, and −2.45 meV for J_2 and 1.89, 1.13, 0.98, 0.80, and 0.69 meV for J_1. They are almost a factor 2 larger in absolute value for J_2 and hence significantly overestimating the Néel temperatures. They are almost an order of magnitude larger for J_1 than obtained here. We find that including Gd $5p$ is crucial to our results. Without it we would find GdN to prefer AFM-II structure. We think however that the main differences from our results with those of Larson and Lambrecht[3] result from their different procedure. Their results for $[111]_1$ were not obtained in the same geometry as the FM state and hence this energy difference was possibly less well converged.

What all calculations and experiment clearly agree on is an increase in $|J_2|$ from P to Bi, directly corresponding to an increase in Néel temperature. Although there is less consensus on the J_1 values, clearly it is a smaller interaction than J_2 and is decreasing from N to Bi. As discussed by Duan *et al.*[5] the effective J_2 interaction can be interpreted as arising from superexchange between Gd d moments induced by the f-d interaction via the intervening anion p states with which they increasingly overlap, the larger the anion size.

The origin of the J_1 interaction however is less clear, and even its sign is not very clear. They interpreted it as RKKY in origin. We examine this proposal in some more detail

TABLE III. Magnetic moments in μ_B.

	FM		AFM-I		AFM-II	
	Gd *d*	Anion	Gd *d*	Anion	Gd *d*	Anion
GdN	0.08	−0.08	0.04	−0.03	0.07	0
GdP	0.06	−0.08	0.07	−0.03	0.11	0
GdAs	0.06	−0.07	0.07	−0.02	0.13	0
GdSb	0.07	−0.08	0.09	−0.03	0.18	0
GdBi	0.07	−0.09	0.11	−0.02	0.20	0

here. Based on the band structures, one expects an increasing overlap of the valence and conduction bands with an increasing carrier concentration in the electron pocket. This will lead to an increase in k_F and hence shorter period for the RKKY oscillations. Assuming a plausible concentration of $n=3\times10^{20}$ e/cm^{-3} and $2k_F=4.1\times10^7$ cm^{-1}. The first minimum of the $\cos 2k_Fr$ RKKY factor then occurs at about 7.6 Å and the sign change at 3.8 Å. We can see that indeed the nearest-neighbor distance between Gd atoms (4.0–4.5 in GdP-GdBi) is then already in the first negative lobe of the RKKY oscillation and increasingly strongly negative for the heavier anion both because the lattice constant increases and because the overlap of the bands and hence carrier concentration increases. This agrees with the results of Duan *et al.*[5] For GdN, the nearest-neighbor distance is 3.5 Å, and the nearest-neighbor exchange would still be positive, perhaps even second-nearest-neighbor RKKY could still be positive if the carrier density is somewhat lower (for example, 1×10^{20} cm^{-3} would give the first zero in $\cos 2k_Fr$ at 5.4 Å). If the band structure is semimetallic there is also a compensating hole pocket. Both electron and hole gases could give rise to RKKY-like interactions and reinforce each other. In our band structures, the band overlap in Gd(P-Bi) can be expected to be reduced compared to that in Duan *et al.*[5] because of our U_d shift, and hence smaller carrier concentrations will result. This will shift the point where exchange interactions become negative to larger distances. Possibly this is the reason why we obtain a small positive J_1 except for Bi. Thus overall, the RKKY model seems plausible as origin for J_1. On the other hand, we would then expect a long-range $1/r^3$ decay while the exchange interactions calculated from first principles are found to fall rather fast. Also, in pure semiconducting GdN, this explanation does not hold because there are no free electrons.

To gain further insight, we inspect the magnetic moments. In Table III, we show our calculated magnetic moment for the three configurations and for each of the materials. These are extracted by integrating the spin density beyond the muffin-tin sphere radius to estimate the true moment per atom. In Gd, we find a magnetic moment slightly larger than the $4f$ value of $7\mu_B$, indicating a Gd $5d$ moment parallel with the $4f$ moment. This arises clearly from the induced spin splitting of the valence bands. This is however a rather subtle effect. Although in GdN both majority and minority-spin bands are completely filled since we have a semiconductor, it must indicate that the valence bands, which have N p-Gd d bonding character must have slightly larger hybridization with the Gd d for the majority spin than for the minority spin. The spins of the top valence and lowest conduction bands are reversed, so indeed the Gd d of majority spin are somewhat closer in energy to the N majority-spin band and hence are expected to have slightly stronger hybridization. In the other pnictides, we have a semimetallic band structure and hence the mainly Gd d bands are partially occupied but only very slightly near the X point of the Brillouin zone. Since the Gd d bands of majority spin are slightly lower than the minority spin, it is somewhat easier to understand a slight positive Gd d moment parallel to the f moment. Since the total moment per Gd in the ferromagnetic state is almost exactly 7 for all cases, it means that a positive Gd d moment must be compensated by an opposite moment on the N. In fact, we are then missing electrons from the majority-spin N-like valence band and hence expect an opposite moment on N. On the other hand, in the AFM-II case, the anion has exactly three nearest-neighbor Gd of one spin on one side and of opposite spin on the other side. In that case, we see that the moment is zero on the anion. In the AFM-I case, we find an intermediate situation with four of its Gd neighbors in the same (001) plane having opposite spin and the two above and below it of parallel spin.

From Table III we see furthermore that the size of the Gd d moment is larger in the AFM-II case than in the FM case for P-Bi and increases in the series from P to Bi. This is consistent with an increasingly favorable AFM-II ground state. On the other hand in GdN, the moment is actually slightly larger in the FM case but is then compensated by an opposite N magnetic moment. The two are exactly opposite in this case which is related to the semiconducting nature of the band structure. Viewed in this way, we can think of GdN as an antiferromagnetic ordering on a rocksalt lattice between N and Gd d magnetic moments. Each Gd is surrounded by six N and vice versa with opposite spins. Because of the f-d coupling to the Gd $4f$, however, this locks all the Gd into a ferromagnetic configuration relative to each other. We could thus say that GdN is an antiferromagnet in disguise. The fact that the stabilization of this peculiar AFM arrangement of spins on N and Gd is preferred in GdN but not in Gd(P-Bi), however, appears to be related to the size of the magnetic moments, in other words due to longitudinal fluctuations of the moments for different arrangements of the spin orientations. This is clearly physics beyond the Heisenberg Hamiltonian, which assumes fixed moments. The Heisenberg Hamiltonian captures the net result for the Gd $4f$ fixed size localized spins but not for the small moments induced on the N and Gd d. The latter in effect represent the induced moments equivalent to the ones induced in the electron gas in RKKY theory. Ultimately, the preference for a FM alignment for GdN is related to the formation of a magnetic moment on the N, whereas the AFM-II state is preferred for the other group-V anions because in that case no magnetic moment forms on the anion. The propensity of N p orbitals to allow for a magnetic moment is well known and has recently been discussed in connection with defect mediated magnetism in magnetic semiconductors.[30] The picture we obtain here for the origin of magnetism is somewhat similar to that proposed by Fang *et al.*[31] for Sr_2FeMO_6 double perovskites with M standing for Mo, Re, or W. In

these materials there is a similar competition between FM and AFM-II configurations and the moments induced on the nominally nonmagnetic element M play a key role.

B. Linear response results

The linear-response theory of Liechtenstein *et al.*[16] provides an attractive alternative approach to studying exchange interactions. In this approach, exchange interactions are calculated as the response to small-angle fluctuations of the spin orientation. The method is formulated in multiple-scattering theory and expresses the exchange interactions in closed form as an integral up to the Fermi energy,

$$J_{ij} = \frac{2}{\pi}\int_0^{\epsilon_F} d\epsilon \ \mathrm{Im\ Tr}\{\delta P_i g_{ij}^{\uparrow} \delta P_j g_{ij}^{\downarrow}\}, \tag{6}$$

where $\delta P_i = (P_i^{\uparrow} - P_i^{\downarrow})/2$, P_i are the LMTO potential functions, corresponding to the cotangent of the phase shift or inverse t-matrix element in multiple-scattering theory, and $\mathbf{g}(\epsilon) = [\mathbf{P}(\epsilon)\delta_{ij} - \mathbf{S}]^{-1}$ is the Green's function, with $\mathbf{S}$ as the structure constants and boldface indicates the matrix structure in the atomic sites, angular momenta, and spin. To use this close relation to multiple-scattering theory in LMTO we need to use the ASA. We thus first need to examine how well this approach reproduces the small energy differences we are here interested in as well as the band structure. In fact, the linear-response approach is based on the magnetic force theorem[16] and thus only uses the changes in occupied one-electron energies, calculated non-self-consistently for frozen changes in potential when rotating the spins. Thus, a correct band structure appears to be crucial.

We find that the latter is sensitive to the choice of sphere radii and when applied directly to self-consistent total-energy differences it is not sufficiently accurate to agree with FP-LMTO. For example, it finds AFM-II to be the ground state for GdN in disagreement with experiment. In order to obtain the correct band splittings, it is necessary to keep the Gd sphere ratio to the anion somewhat smaller than expected on the basis of their atomic radii.[32] We here use s/w values of 1.159, 1.159, and 0.762 for Gd, anion, and empty sphere, respectively, with s as the sphere radius of each species and w as the average Wigner-Seitz sphere radius. Otherwise, we find that the interaction between Gd f and N p is suppressed and the splitting of the valence bands reverses. We also use a slightly larger $U_f - J_f$ value of 8 eV, chosen so as to reproduce the FP-LMTO band structures as faithful as possible. In spite of these careful adjustments, the direct self-consistent total-energy differences were not in agreement with the FP-LMTO. However, when we apply the magnetic force theorem, most of the terms in the Kohn-Sham total energy cancel and we only need the one-electron band structure to be accurate.

In Fig. 1 we show the energy difference obtained in a $[001]_1$ cell upon rotating the spin on the second layer by an angle θ relative to the spin on the first layer, calculated with rigid potentials and using Gd $5p$ orbitals. We can see that the energy cost of rotating the spin by π corresponding to the energy difference between AFM-I and FM is 5.5 meV/pair. This is only slightly larger than the FP-LMTO result (3.4 meV/pair) and slightly lower than Duan *et al.*[5] (6.7 meV/pair). We can see that the $(1-\cos\theta)$ behavior of the Heisenberg Hamiltonian is well obeyed.

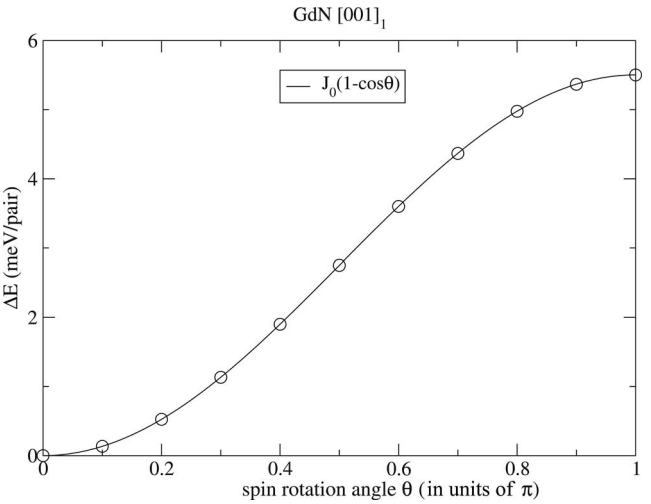

FIG. 1. Energy change in $[001]_1$ cell upon rotating spins of layer 2 relative to that in layer 1.

Next, we use the Green's function linear-response approach to decompose this energy difference into its individual atom exchange interactions. For GdN, we treat the Gd $5p$ as bands because of the smaller lattice constant while for the other pnictides, we treat Gd $5p$ as core and Gd $6p$ as band. Also for the other materials, we perform the linear-response calculation around the antiferromagnetic AFM-II ground state. We find the exchange interactions given in Table IV.

Longer-range interactions are essentially zero. We focus first on GdN. We note that the exchange interactions with empty sphere and N are actually comparable in magnitude with those between Gd directly. Inspecting the magnetic moments, we find that with these sphere sizes, the net magnetic moment per Gd sphere is $6.97 = 7 - 0.03\mu_B$, $-0.005\mu_B$ on N, and $0.0175\mu_B$ on empty spheres. What this means is that the empty spheres in some sense represent the tails of the Gd d orbitals. Restoring their moment to Gd, we would arrive at a net Gd d moment of $0.005\mu_B$. More particularly because of their location relative to the Gd sphere, the empty spheres can be thought of as representing the tail of the t_{2g} orbitals. Viewed in this way, the structure looks like a bcc lattice with empty spheres in the center surrounded by four Gd and four

TABLE IV. Exchange interactions in Gd-pnictides (in meV) calculated in linear response using FM ground state for GdN and Gd $5p$ as band, and AFM-II as ground state and Gd $6p$ as band for the other cases.

	J_1(Gd-Gd)	J_2(Gd-Gd)	J_1(Gd-N)	J_1(Gd-E)
GdN	0.272	0.190	0.136	0.218
GdP	0.163	−0.707	0	0.081
GdAs	0.136	−0.843	0	0.082
GdSb	0.218	−1.143	0	0.054
GdBi	0.789	−1.714	0	0.082

N spheres. If we ignore the large $4f$ moment on the Gd, we find again an antiferromagnetic or rather ferrimagnetic arrangement of the moments on empty spheres surrounded by opposite moments on the Gd and N spheres.

We can see that if we add up all the exchange interactions connecting to the Gd atom, a total $J_0=\Sigma_i J_{0i}$ of 6.96 meV is obtained. This is twice the energy difference ΔE_I and is close to the result of the noncollinear calculation and even closer to the FP-LMTO result. It gives a mean field T_c(MF) $=J_0/3k_B$ of 27 K. But of course, we now have also to consider the net J_0 connected to N and empty spheres. They have smaller J_0 of 0.8 and 0.9 meV leading to a net average T_c of about 10 K. This is in good agreement with the FP-LMTO calculation.

We can further examine how J_0 on each site is distributed over angular momentum. This shows that on Gd, the f orbitals contribute only 0.4 meV, $d(e_g)$ contribute 3.2 meV, $d(t_{2g})$ 3.5 meV, Gd $5p$ −0.4 meV, N p 0.9 meV, the empty sphere s 0.8, and p 0.2 meV. These numbers agree with the decomposition in individual atom pairs to ± 0.1 meV. The slight deviations are because of rounding. It confirms that the f electrons play a rather unimportant role in establishing the magnetic ordering. Their magnetic moments are just too localized to give any direct interactions with neighbors. Rather, their role is to induce a moment on Gd d via f-d coupling, which then for the e_g orbitals couple to the neighbors via t_{pd} hopping to N p and for the t_{2g} orbitals directly between Gd nearest neighbors via t_{dd} hopping or in the present scheme via empty spheres. The indirect coupling of Gd second-nearest neighbors via N p is what gives rise to the superexchange. If we lump the empty sphere contribution together with the t_{2g} orbitals, we see that the latter give a sizable net nearest-neighbor interaction of about 5.5 meV or 0.46 meV/neighbor. This is close to what the FP-LMTO tells us the net Heisenberg interaction is between nearest-neighbor Gd atoms.

It corresponds to a rather different view on how the induced spin density is distributed in space and hence how their net interactions are accounted for in a corresponding Heisenberg-type Hamiltonian, which would now include spins on all sites, not just the Gd sites. Nonetheless, it ultimately arrives at the same mean-field Curie temperature. It shows us that the exchange interactions as written between Gd $4f$ spins are just some renormalized effective interaction arising from the multiple type of exchange interactions between N p, Gd d, and spin density located in the empty spheres. This is actually not too unlike the physical picture of the RKKY model. In the latter, moments are induced in the electron gas and provide indirect interactions between Gd f. Here moments are induced on the Gd d and neighboring sites which then have exchange interactions with each other. The advantage of the present point of view is that it does not require a net free-carrier concentration. We should rather think about it as some type of itinerant interactions between the d and N orbitals. Importantly, we see that for GdN, this leads to what is in effect an antiferromagnetic arrangement between the induced moments on N and on Gd d as is expected for a semiconductor.

For GdP, GdAs, GdSb, and GdBi, the linear-response calculations show negligible contribution from Gd-anion and Gd-empty sphere exchange interactions. J_1 and J_2 are comparable to those obtained in the FP-LMTO calculation. When considering only the Gd atoms, we obtain a T_N(MF) of 16.4 K for GdP, i.e., 14% lower than the FP-LMTO calculation but this is not surprising given the additional approximations in the band-structure calculation and the totally different approach. If we calculate exchange interactions as linear response around the FM state, we obtain $J_1=0.082$ meV and $J_2=-0.626$ meV, which qualitatively is still consistent with the calculation around the actual ground state but obviously less accurate. Similar results apply for GdAs, GdSb, and GdBi. From the J_2 values in Table IV we obtain as mean-field Néel temperatures 16.4, 19.6, 26.5, and 39.8 K for GdP, GdAs, GdSb, and GdBi, respectively, or 11.5, 13.7, 18.5, and 27.9 as best estimates using $0.7T_N$(MF). These are in fair agreement with the FP-LMTO results and reproduce the correct trend.

C. Further discussion of GdN

While for Gd(P-Bi) we obtained good agreement with experimental values for the Néel temperature, the estimates we obtain for the Curie temperature for GdN of about 10 K are much smaller than estimated before and significantly lower than the experimental values (58–70 K). This raises the question to what extent carrier mediated and/or defect mediated magnetism may play a role in GdN. Within the linear-response approach, we can test the effect of carriers directly by simply changing the Fermi level. This assumes a rigid-band picture. We find that by shifting the Fermi level inside the conduction band with carrier concentrations up to about 4×10^{20} cm^{-3}, corresponding to a Fermi level of 0.6 above the conduction-band minimum, the exchange interactions did not change appreciably and T_c stayed the same. For higher concentrations, say, E_F 1.4 eV above the conduction-band minimum and carrier concentration 5.6×10^{21} cm^{-3}, we find J_2 to decrease to zero and longer range negative contributions start to come in, leading to a lower T_c of only 3.9 K. For even higher concentrations, the antiferromagnetic interactions become dominant. On the other hand, a 3×10^{21} p-type doping corresponding to E_F of 81 meV below the valence-band maximum (VBM) gave an increased T_c of 23.8 K. In practice p-type doping seems unlikely in GdN and such high carrier concentrations that lead to the AFM lobe of the RKKY-like coupling also seem implausible. Thus, it seems that the relatively high experimental Curie temperature of GdN cannot be explained simply in terms of carrier mediated coupling in a rigid-band picture. We need to include the defect induced changes in the band structure explicitly. As the nature of these defects is presently not clear and large cell simulations are required, we reserve this for a future study. We only remark that for metallic Gd in the hcp structure using the same ASA linear-response approach and including all $J_{ij}\leq 0.02$ mRyd, we obtain a mean field T_c(MF) of 406 K. Using our usual rule of thumb that the real critical temperature is 30% lower, we obtain 285 K, rather close to the experimental value of about 297 K. Thus the method seems to be capable of describing the exchange interactions of Gd systems from Gd X with X=P, As, Sb, and Bi to pure Gd but

nevertheless fails to give the experimental values for GdN by almost an order of magnitude.

IV. CONCLUSIONS

In this paper we revisited the calculation of exchange interactions in Gd pnictides. We used both FP-LMTO and ASA Green's function linear-response calculations. LSDA+U is used with both U_f and U_d. U_f is introduced to obtain a splitting of empty and filled f states in agreement with experiment and U_d is introduced to obtain a gap in GdN, in agreement with recent experimental data.[8]

For GdP, GdAs, GdSb, and GdBi, the Heisenberg Hamiltonian with only first- and second-nearest-neighbor interactions between Gd atoms gives an accurate description of the magnetic properties. Our large basis set FP-LMTO results agree better with the results of Duan *et al.*[5] than with Larson and Lambrecht.[3] They predict Néel temperatures to within about 20% of experimental values and also obtain negative Curie-Weiss temperatures in good agreement with experimental data by Li *et al.*[1] Linear response calculations within ASA around the AFM-II ground state get these same interactions to within a few percent. The trend in this series of antiferromagnets clearly arises from the increasing overlap of the anion p orbitals with the Gd d and as previously shown by Duan *et al.*[5] can be understood as superexchange between the magnetic moments induced on the Gd d orbitals. We find the nearest-neighbor interaction to be somewhat smaller in absolute value and positive. This can be understood qualitatively from an RKKY point of view as resulting from our smaller band overlap in these semimetals. Alternatively, however, we can view these nearest-neighbor interactions as simply arising from the direct exchange interactions between induced Gd d orbital moments. We also find that in the AFM-II structure, the magnetic moment on the anion is exactly zero, whereas in a FM configuration, the magnetic moment on Gd d is slightly smaller and opposed by an opposite N induced moment. Ultimately, the preference for the AFM-II structure is related to its slightly larger Gd d moments which hence provide a stronger coupling.

In GdN, on the other hand, we find the FM structure to be preferred because it has slightly larger magnetic moments on the Gd d than in the AFM-II structure. This FM structure can be alternatively viewed as an AFM ordering of the Gd d and N magnetic moments of opposite sign on the rocksalt lattice. It pins the Gd f local moments in a ferromagnetic configuration through the on-site f-d exchange. The resulting net exchange interactions between Gd atoms are positive for both nearest and second-nearest neighbors but significantly smaller than previous calculations indicated, leading to a mean-field Curie temperature of only about 10 K. Linear response calculations show that in GdN, exchange interactions between the moments induced on N and on empty sphere sites are of comparable magnitude as the ones between Gd d atoms. The empty sphere may be viewed as representing the tails of the Gd t_{2g} orbitals. The decomposition of the total exchange interaction in angular components reveals directly that f electrons give only a small contribution. Their role is only to induce the moments on Gd d and the neighbors and the magnetism arises from direct interactions between those induced moments. Importantly, this picture does not require a net free-carrier concentration to mediate interactions between Gd atoms and is thus consistent with the semiconducting nature of GdN. The very small Curie temperature obtained here for pure GdN disagrees with experimental findings of a Curie temperature of about 58–70 K.[1,7–10] This suggests extrinsic origins for this observed Curie temperature. Linear response calculations show that carrier mediated coupling via conduction electrons n-type doping does not change the Curie temperature much and in fact would start decreasing the Curie temperature even further for large enough n-type doping. This suggests that defect states, such as possibly N vacancies, play a more direct role than simply providing mobile carriers. Further evidence for this is found in the fact that the approach gives a reasonable value for the Curie temperature of metallic Gd.

ACKNOWLEDGMENTS

We thank A. G. Petukhov and Mark van Schilfgaarde for useful discussions. This work was supported by the National Science Foundation World Materials Network Grant No. DMR-0710485.

[1] D. X. Li, Y. Haga, H. Shida, T. Suzuki, Y. S. Kwon, and G. Kido, J. Phys.: Condens. Matter **9**, 10777 (1997).
[2] T. Kasuya and D. X. Li, J. Magn. Magn. Mater. **167**, L1 (1997).
[3] P. Larson and W. R. L. Lambrecht, Phys. Rev. B **74**, 085108 (2006).
[4] C.-G. Duan, R. F. Sabiryanov, J. Liu, W. N. Mei, P. A. Dowben, and J. R. Hardy, Phys. Rev. Lett. **94**, 237201 (2005).
[5] C.-G. Duan, R. F. Sabiryanov, W. N. Mei, P. A. Dowben, S. S. Jaswal, and E. Y. Tsymboal, Appl. Phys. Lett. **88**, 182505 (2006).
[6] D. B. Ghosh, M. De, and S. K. De, Phys. Rev. B **72**, 045140 (2005).
[7] S. Granville *et al.*, Phys. Rev. B **73**, 235335 (2006).
[8] H. J. Trodahl, A. R. H. Preston, J. Zhong, B. J. Ruck, N. M. Strickland, C. Mitra, and W. R. L. Lambrecht, Phys. Rev. B **76**, 085211 (2007).
[9] F. Leuenberger, A. Parge, W. Felsch, K. Fauth, and M. Hessler, Phys. Rev. B **72**, 014427 (2005).
[10] F. Leuenberger, A. Parge, W. Felsch, F. Baudelet, C. Giorgetti, E. Dartyge, and F. Wilhelm, Phys. Rev. B **73**, 214430 (2006).
[11] M. Methfessel, M. van Schilfgaarde, and R. A. Casali, in *Electronic Structure and Physical Properties of Solids: The Use of the LMTO Method*, Lecture Notes in Physics Vol. 535, edited by H. Dreyssé (Springer-Verlag, Berlin, 2000), p. 114.
[12] J. Zaanen and G. A. Sawatzky, Can. J. Phys. **65**, 1262 (1987).
[13] M. A. Ruderman and C. Kittel, Phys. Rev. **96**, 99 (1954).

[14] T. Kasuya, Prog. Theor. Phys. **16**, 45 (1956).
[15] K. Yosida, Phys. Rev. **106**, 893 (1957).
[16] A. I. Liechtenstein, M. I. Katsnelson, V. P. Antropov, and V. A. Gubanov, J. Magn. Magn. Mater. **67**, 65 (1987).
[17] P. Hohenberg and W. Kohn, Phys. Rev. **136**, B864 (1964).
[18] W. Kohn and L. J. Sham, Phys. Rev. **140**, A1133 (1965).
[19] U. von Barth and L. Hedin, J. Phys. C **5**, 1629 (1972).
[20] V. I. Anisimov, J. Zaanen, and O. K. Andersen, Phys. Rev. B **44**, 943 (1991).
[21] A. I. Liechtenstein, V. I. Anisimov, and J. Zaanen, Phys. Rev. B **52**, R5467 (1995).
[22] P. Larson, W. R. L. Lambrecht, A. Chantis, and M. van Schilfgaarde, Phys. Rev. B **75**, 045114 (2007).
[23] H. Yamada, T. Fukawa, T. Muro, Y. Tanaka, S. Imada, S. Suga, D.-X. Li, and T. Suzuki, J. Phys. Soc. Jpn. **65**, 1000 (1996).
[24] O. K. Andersen, Phys. Rev. B **12**, 3060 (1975).
[25] O. K. Andersen and O. Jepsen, Phys. Rev. Lett. **53**, 2571 (1984).
[26] O. K. Andersen, Z. Pawlowska, and O. Jepsen, Phys. Rev. B **34**, 5253 (1986).
[27] O. K. Andersen, T. Saha-Dasgupta, R. W. Tank, C. Arcangeli, O. Jepsen, and G. Krier, in *Electronic Structure and Physical Properties of Solids: The Use of the LMTO Method*, Lecture Notes in Physics Vol. 535, edited by H. Dreyssé (Springer-Verlag, Berlin, 2000), pp. 3–84.
[28] V. P. Antropov, M. I. Katsnelson, B. N. Harmon, M. van Schilfgaarde, and D. Kusnezov, Phys. Rev. B **54**, 1019 (1996).
[29] D. Singh, Phys. Rev. B **43**, 6388 (1991).
[30] P. Dev, Y. Xue, and P. Zhang, Phys. Rev. Lett. **100**, 117204 (2008).
[31] Z. Fang, K. Terakura, and J. Kanamori, Phys. Rev. B **63**, 180407(R) (2001).
[32] C. Mitra and W. R. L. Lambrecht, Phys. Rev. B (to be published).